

# WDiscOOD: Out-of-Distribution Detection via Whitened Linear Discriminative Analysis

Yiye Chen Yunzhi Lin Ruinian Xu Patricio A. Vela  
Georgia Institute of Technology

{yychen2019, yunzhi.lin, rnx94, pvela}@gatech.edu

## Abstract

Deep neural networks are susceptible to generating overconfident yet erroneous predictions when presented with data beyond known concepts. This challenge underscores the importance of detecting out-of-distribution (OOD) samples in the open world. In this work, we propose a novel feature-space OOD detection score that jointly reasons with both class-specific and class-agnostic information. Specifically, our approach utilizes Whitened Linear Discriminative Analysis to project features into two subspaces - the discriminative and residual subspaces - in which the ID classes are maximally separated and closely clustered, respectively. The OOD score is then determined by combining the deviation from the input data to the ID distribution in both subspaces. The efficacy of our method, named WDiscOOD, is verified on the large-scale ImageNet-1k benchmark, with six OOD datasets that covers a variety of distribution shifts. WDiscOOD demonstrates superior performance on deep classifiers with diverse backbone architectures, including CNN and vision transformer. Furthermore, we also show that our method can more effectively detect novel concepts in representation space trained with contrastive objectives, including supervised contrastive loss and multi-modality contrastive loss.

## 1. Introduction

Deep learning models are typically designed under the *closed-world* assumption [44], in which the test data is assumed to be drawn from the same distribution as the training data. Without any built-in mechanism to distinguish novel concepts, deep neural networks are prone to generate incorrect answer with high confidence when presented with *out-of-distribution (OOD)* data. Such a misleading decision could result in catastrophic consequences in certain applications, which makes the deep neural network hard to deploy in the *open world*. To address this issue, significant research efforts have been devoted to the problem of OOD

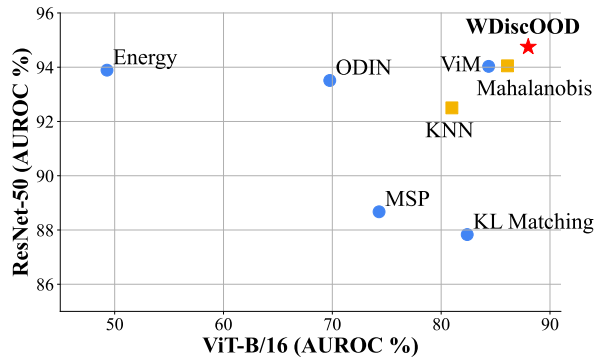


Figure 1: **Performance on two OOD detection benchmarks.** We propose a novel OOD detection method based on *Whitened Linear Discriminative Analysis*, which is highlighted with red star. It outperforms baselines with both ResNet-50 (x-axis) and ViT-B/16 (y-axis) model on ImageNet-1k benchmark. Blue dots and yellow square denote classifier-based and feature-based methods, respectively. The AUROCs are averaged over six OOD datasets, for which the detailed results are tabulated in Tab. 1.

detection, which aims to establish a robust method for identifying when the testing data is “unknown”.

Specifically, OOD detection problem requires to establish a scoring function to separate ID and OOD data. Designed for deep visual classifiers, the major line of work examines the activity pattern from the classification layer. For example, a popular baseline is to leverage the maximum posterior probability output by softmax classifier to indicate ID-ness [20], assuming that the network is more confident with its decision for ID data. The idea is enhanced by neural network calibration research [16, 31, 23], which aims to align network confidence with true correctness likelihood. The technique has been shown to improve OOD detection performance. Other classifier-based scores explore unnormalized posterior probability known as logit [19, 32], and norm of gradients backpropagated from classification layer outputs [24, 28].

Recently, ViM [42] argues that both class-dependent and class-agnostic information can potentially facilitate the OOD detection task. Based on the idea, it designs a scoring function by mapping the feature residual from the principle

components to the logit space. Despite the great performance achieved, ViM still requires access to a supervised classification layer. In the meantime, recent years have seen significant advances in pretraining large-scale visual encoders using contrastive learning techniques [3, 26]. These methods no longer rely on being jointly trained with task heads, but instead formulate objectives directly in the feature space to produce high-quality visual representations. It is shown that the learnt encoder can be applied to downstream tasks with little or no fine-tuning required [35, 37], suggesting a new trend in the paradigm for solving vision tasks. While it is non-trivial to adopt classifier-based OOD detection methods directly to visual encoders, applying feature space methods is straightforward. For example, SSD [36] applies Mahalanobis [30] distance on the contrastive feature space, which demonstrates superior performance compared to vanilla classification visual encoder.

In this work, we aim to reason about both class-specific and class-agnostic information *solely within the feature space*. To achieve this, we utilize Whitened Linear Discriminative Analysis (WLDA) to project visual features into two subspaces: a discriminative subspace and a residual subspace. The former contains compact class-discriminative signals, while the latter constrains shared information. We refer to these subspaces as Whitened Discriminative Subspace (WD) and Whitened Discriminative Residual Subspace (WDR), respectively. Given the compactness of the WD space, we detect anomalies by measuring the distance to the nearest class center. Conversely, in the WDR space where in-distribution (ID) classes are entangled, we design the out-of-distribution (OOD) score as the distance to the centroid of all training data. The final proposed scoring function unifies the information from both subspaces by computing a weighted sum of the scores in each space.

While subspace techniques for OOD detection have been explored by previous literature [5], our approach differs significantly. Assuming ID data lies on a low-dimensional manifold, existing approaches measure the residual magnitude as an indicator for OOD-ness [33]. In contrast, we assume the residual space captures rich class-shared information. Furthermore, while past literature examines the residual to principles [42] or classifier weights [5], we explore the remaining information to discriminative components. This design enables us to jointly reason with both discriminative and residual information without relying on task heads, which is more applicable to stand-alone visual encoders.

As shown in Fig. 1, WDiscOOD achieves superior performance on large-scale ImageNet-1k benchmark compared to a wide range of baselines, under both classic CNN and recent Visual Transformer (ViT) architectures. In addition, our method surpasses other feature-space approaches in distinguishing novel concepts from stand-alone con-

trastive encoders, involving Supervised Contrastive (SupCon) model [26] and Contrastive Language-Image Pre-Training (CLIP) model [35]. What’s more, we discover that the Whitened Discriminative Residual Space is more effective in identifying anomaly responses compared to other subspace techniques or even a subset of classifier-based scoring methods, verifying the importance of class-agnostic feature component for the task.

In summary, our contribution involves:

- A new OOD detection score, based on WLDA, that jointly considers class-discriminative and class-agnostic information solely within the feature space.
- A new insight into the effectiveness of the Whitened Discriminative Residual Subspace space, which captures the shared information stripped of discriminative signals, for detecting anomalies in OOD samples.
- New state-of-the-art results achieved by our method on the large-scale ImageNet OOD detection benchmark, for various visual classifiers (CNN and ViT) as well as contrastive visual encoders (SupCon and CLIP).

## 2. Related Work

**Scoring Functions for Pretrained Models** One line of work explores scoring functions to distinguish inliers and outliers, which is fundamental for the OOD detection task. Multiple designs have been proposed for pretrained deep visual classifiers [1, 27, 20, 32, 19, 24, 28, 38, 42, 33, 30, 39]. The most straightforward design is Maximum Softmax Probability (MSP) score, which considers the network confidence as an uncertainty measurement. ODIN [31] improves MSP’s performance via two calibration techniques - input preprocessing and temperature scaling. Logit-space methods involve max logit [19] and energy score [32]. The latter is further enhanced by feature rectification [32]. Huang et al. [24] and Lee et al. [28] investigate gradient space, which demonstrates effectiveness in revealing ID and OOD distinction. Those methods achieve great performance on several OOD detection benchmarks, but are tailored to the classification task and not applicable to pretrained visual encoders since they are dependent on classifier outputs. On the other hand, methods based on feature space analysis, such as Mahalanobis [30] and KNN [39], not only exhibit exceptional OOD detection performance for classification models, but also showcase applicability to stand-alone visual encoders, including SupCon [26, 36] and CLIP [35, 14]. Subspace analysis [42, 33, 5] measures the residual information from low-dimensional manifold [33] or column space of classifier weights. However, to achieve state-of-the-art performance, the result needs to be converted to classifier output space to factor in class-dependent information [42]. In this work, we combine the

residual and discriminative information solely in the feature space via Linear Discriminative Analysis, which makes our method applicable on any visual encoder.

**Model Modifications & Training Constraints** Another branch of OOD detection methods trains the network to respond differently to ID and OOD data, by either modifying the network structure [23] or adding specialized training regularization [25, 46, 45]. Along with this thread, the most direct approach is to encourage the network to give distinguishable predictions for outlier data, such as uniform posterior probability [21], lower energy [32], or confidence estimation from dedicated branch [7]. Such a training typically incurs the requirement for auxiliary OOD training set, or commonly known as Outlier Exposure (OE) [21]. Several methods [8, 21] assume the availability of unknown data from outlier datasets, which can hardly cover all potential distribution shifts in the open world, and is not always feasible. Lee et al. [29] utilizes generative model, such as Generative Adversarial Networks (GAN) [15] for outlier data synthesis. However, generating high fidelity image induces difficulty for optimization. To avoid the obstacle, VOS [11] proposes to synthesize outliers in the feature space, which can be adaptive to the ID feature geometry during training. Although effective, these methods require network re-training to endow the model with the ability to reject OOD data, which can be expensive and intractable especially for models trained on large-scale datasets. On the other hand, our OOD scoring function design can be directly applied on any pre-trained visual model.

### 3. Methods

The core of OOD detection lies in creating a scalar function  $s(\cdot)$  that assigns distinguishable scores to ID and OOD data. This allows the query data to be classified as either ID or OOD by applying a threshold to the score. In this paper, we aim to assign higher scores for ID data. Our approach involves disentangling class-discriminative and class-general information from the feature of the penultimate layer in the network using Whitened Linear Discriminative Analysis. We then jointly reason with both types of information to effectively identify OOD data. We first introduce LDA in Sec.3.1, and then explain the proposed WDiscOOD score based on LDA in Sec. 3.2 .

#### 3.1. Multiclass Linear Discriminative Analysis

The objective of Linear Discriminative Analysis (LDA) [13, 12] is to find a set of projection directions, termed *discriminants*, along which multi-class data are maximally separated. Specifically, given a training dataset  $\{(x_i \in \mathbb{R}^D, y_i)\}_i^N$  of  $D$ -dimensional features from  $C$  classes ( $y_i \in \{1, 2, \dots, C\}$ ), the objective of LDA is to find the direction

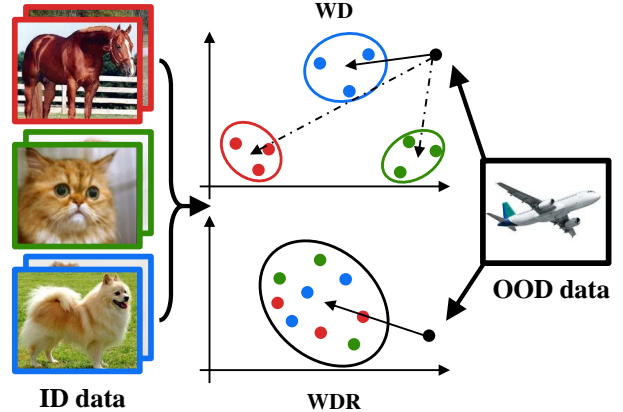


Figure 2: **Overview of WDiscOOD method.** It detects an OOD sample by projecting the feature into *Whitened Discriminative Subspace (WD)* and *Whitened Discriminative Residual Subspace (WDR)*, where ID classes are maximally separated and closely cluttered, respectively. Based on this, we assume that OOD samples are further away from either all class clusters in the WD space or the entire dataset clutter in the WDR space. Therefore, we formulate the OOD score as a combination of the distance towards the nearest class centroid in the WD space and towards the entire dataset centroid in the WDR space.

$w$  such that the *Fisher discriminant criterion* [2], defined as the ratio of inter-class variance over intra-class variance, is maximized:

$$\max_w J(w) = \frac{w^T S_b w}{w^T S_w w} \quad (1)$$

where  $S_b$  and  $S_w$  are between-class scatter matrix and within-class scatter matrix. Denote the cardinality for class  $c$  as  $N_y$ , the scatter matrices are formulated as:

$$S_w = \sum_{i=1}^N (x_i - \mu_{y_i})(x_i - \mu_{y_i})^T \quad (2)$$

$$S_b = \sum_{c=1}^C N_c (\mu_c - \mu)(\mu_c - \mu)^T \quad (3)$$

where  $\mu$  is defined as the center of entire training dataset.

The optimization of Eq. 1 can be done by solving the generalized eigenvalue problem:

$$S_b w = \lambda S_w w \quad (4)$$

where the generalized eigenvalue is equal to Fisher criterion for the corresponding eigenvector. Intuitively, a larger Fisher criterion suggests that ID classes are better separated. Therefore, projecting original features onto top discriminants, known as *Foley-Sammon Transform (FST)*, maps the original feature to a low-dimensional subspace where ID classes are compactly clustered. As described in the following section, we utilize FST to disentangle discriminative and residual information from visual feature space.

### 3.2. WDiscOOD: Whitened Linear Discriminative Analysis for OOD detection

As shown in Fig. 2, given extracted image feature  $\mathbf{z}$ , our proposed WDiscOOD score involves three steps: (1) data whitening with the statistics derived from the training dataset; (2) discriminative and residual space mapping with discriminants and discriminant orthogonal complement set, which are estimated based on LDA; (3) weighted sum of distance towards ID cluster in both spaces as the final WDiscOOD score.

**Data Whitening** We begin by whitening the feature prior to conducting LDA. The application of whitened LDA has been extensively studied and implemented across various domains [34, 17]. According to Hariharan et al. [17], data whitening eliminates the correlation between feature elements and enhances the feature’s capability to encode data similarity. Furthermore, it improves numerical condition of LDA, particularly in scenarios involving limited number of samples. In this paper, we whiten the feature with within-class covariance matrix from Eq. 2. Suppose the eigenvalue decomposition for the covariance matrix on the feature space:  $\mathbf{S}_{\mathbf{z}, \mathbf{w}} = \mathbf{V}_{\mathbf{w}} \mathbf{\Lambda}_{\mathbf{w}} \mathbf{V}_{\mathbf{w}}^T$ , where  $\mathbf{V}_{\mathbf{w}} \in \mathbb{R}^{D \times r}$ ,  $\mathbf{\Lambda}_{\mathbf{w}} \in \mathbb{R}^{r \times r}$ ,  $r$  denotes matrix rank, then the feature is whitened by:

$$\mathbf{x} = \mathbf{S}_{\mathbf{z}, \mathbf{w}}^{-1/2} \mathbf{z} = \mathbf{V}_{\mathbf{w}} \mathbf{\Lambda}_{\mathbf{w}}^{-1/2} \mathbf{V}_{\mathbf{w}}^T \mathbf{z} \quad (5)$$

**Discriminative and Residual Space Mapping** In order to isolate the class-specific and class-agnostic components of the whitened visual feature, we leverage LDA to project the data onto two distinct subspaces. The first subspace, which we refer to as *Whitened Discriminative Subspace (WD)*, encodes the discriminative information of the data by compactly grouping samples from the same class and separating different classes. In contrast, the second subspace, which we refer to as *Whitened Discriminative Residual Subspace (WDR)*, captures the residual of the discriminative information by clustering together samples from all classes.

Following [9], we solve LDA by adding a multiple of identity matrix to the within-class scatter matrix  $\mathbf{S}_w + \lambda \mathbf{I}$ . It stabilizes small eigenvalues and ensure the scatter matrix to be well-conditioned. Then the generalized eigenvalue problem in Eq. 4 can be converted to a vanilla eigenvalue problem:

$$(\mathbf{S}_w + \lambda \mathbf{I})^{-1} \mathbf{S}_b \mathbf{w} = \lambda \mathbf{w} \quad (6)$$

With discriminants solved from LDA, we project the feature into WD via Foley-Sammon Transformation. To be specific, we construct the projection matrix  $\mathbf{W} = [\mathbf{w}_1, \mathbf{w}_2, \dots, \mathbf{w}_{N_D}] \in \mathbb{R}^{D \times N_D}$  by stacking the top  $N_D$  discriminants that correspond to the largest Fisher criterion. Then

the WD projection can be obtained by:

$$g(\mathbf{x}) = \mathbf{W}^T \mathbf{x} \quad (7)$$

To capture the class-agnostic information, we project the data onto the subspace that is spanned by the orthogonal complements of the top- $N_D$  discriminants, or what we refer to as the WDR space. The orthogonal complements correspond to projection directions with lower Fisher criterion values, which implies that the separation between classes is less significant compared to intra-class variance. Thus, WDR space captures the shared information among the ID classes, which can be used to formulate additional constraints for ID data. Formally, suppose the eigendecomposition:  $\mathbf{W} \mathbf{W}^T = \mathbf{Q} \mathbf{\Lambda}_w \mathbf{Q}^T$ , then the WDR projection of query feature can be done by:

$$h(\mathbf{x}) = (\mathbf{I} - \mathbf{Q} \mathbf{Q}^T) \mathbf{x} \quad (8)$$

**WDiscOOD Score** The WDiscOOD score combines ID data constraints in both WD and WDR spaces. In the discriminative subspace, where discrepancy between known classes is maximized, all ID data is in close proximity to one of the class clusters. Hence, we formulate WD space OOD detection score as the distance towards the nearest class center  $\mu_c^{WD}$ :

$$s_g(\mathbf{x}) = -\min_c \|g(\mathbf{x}) - \mu_c^{WD}\|_2 \quad (9)$$

In contrast, in the WDR space where inter-class discrepancy is minimized, the data from ID classes tends to scatter around a shared centroid. Thus we measure the OOD score in WDR space as the distance towards the center of all ID training data, which we refer to as  $\mu^{WDR}$ :

$$s_h(\mathbf{x}) = -\|h(\mathbf{x}) - \mu^{WDR}\|_2 \quad (10)$$

The design is distinct from residual norm score from prior work [42, 33], which assumes minimal information left from ID data that is irrelevant for the classification task. Instead, we assume that the residual space contains abundant shared information, motivating us to formulate the distance-based score in Eq. 10.

To factor in the information from both spaces, the final WDiscOOD score is simply defined as the weighted sum of both scores:

$$s(\mathbf{x}) = s_g(\mathbf{x}) + \alpha s_h(\mathbf{x}) \quad (11)$$

## 4. Experiments

In this section, we compare our approach with state-of-the-art methods on large-scale OOD detection benchmarks to demonstrate the effectiveness of our idea. The evaluation is done on both visual classifiers and stand-alone constrative visual encoders. We further provide insights to our method with comprehensive ablation study.

Method	Textures		SUN		Places		iNaturalist		ImgNet-O		OpenImg-O		Average	
	FPR95↓AUROC↑													
<b>Classifier-dependent methods</b>														
MSP [20]	72.98	74.92	70.98	78.75	<u>73.43</u>	76.65	60.90	84.40	95.65	53.13	69.73	81.17	73.94	74.84
Energy [32]	95.74	48.60	97.93	50.12	<u>97.77</u>	48.90	98.12	50.86	92.80	48.23	95.41	52.33	96.30	49.84
ODIN [31]	75.94	69.33	75.51	74.05	<u>77.54</u>	71.28	68.60	79.88	94.95	51.19	73.98	76.15	77.75	70.31
MaxLogit [19]	75.92	69.33	75.51	74.05	<u>77.55</u>	71.28	68.57	79.88	94.95	51.19	73.97	76.15	77.74	70.31
KLMatch [19]	57.57	86.09	70.36	<u>82.91</u>	74.04	<u>80.65</u>	46.83	90.81	89.75	68.86	58.21	88.31	66.13	82.94
ReAct [38]	98.05	34.51	99.66	<u>23.68</u>	99.80	22.86	100.00	23.13	99.40	37.31	99.86	23.86	99.46	27.56
ViM [42]	<u>25.18</u>	<u>92.63</u>	<u>69.22</u>	81.39	74.90	76.40	<u>30.02</u>	<u>93.38</u>	<u>76.15</u>	<u>77.08</u>	<u>46.70</u>	<u>88.60</u>	<u>53.70</u>	<u>84.91</u>
<b>Feature space methods</b>														
Maha [30]	31.17	91.62	<u>66.29</u>	<u>84.31</u>	<u>70.27</u>	<u>81.45</u>	<u>25.64</u>	<u>95.38</u>	<u>81.45</u>	<u>75.65</u>	<b>44.36</b>	<b>91.41</b>	53.20	86.64
KNN [39]	<b>23.26</b>	<b>93.11</b>	88.59	74.01	89.00	71.07	74.60	85.83	<b>71.05</b>	<b>81.15</b>	70.29	84.01	69.47	81.53
<b>WDiscOOD</b>	<u>29.20</u>	<u>91.90</u>	<b>56.83</b>	<b>86.74</b>	<b>64.40</b>	<b>83.13</b>	<b>22.39</b>	<b>95.59</b>	81.60	75.52	<u>44.67</u>	<u>90.51</u>	<b>49.85</b>	<b>87.23</b>

(a) ResNet-50 [18].

Method	Textures		SUN		Places		iNaturalist		ImgNet-O		OpenImg-O		Average	
	FPR95↓AUROC↑													
<b>Classifier-dependent methods</b>														
MSP [20]	52.43	85.42	53.22	86.93	<u>57.75</u>	85.72	13.66	97.00	51.75	85.81	31.99	92.48	43.47	88.89
Energy [32]	36.13	91.25	<u>34.44</u>	<u>93.28</u>	<b>42.80</b>	<b>90.98</b>	5.60	98.94	<u>30.30</u>	93.36	16.06	96.87	27.56	94.11
ODIN [31]	38.57	90.86	37.45	92.81	44.68	<u>90.66</u>	6.03	98.81	33.50	92.69	17.83	96.54	29.68	93.73
MaxLogit [19]	38.56	90.86	37.45	92.81	44.68	<u>90.66</u>	6.03	98.81	33.50	92.69	17.83	96.54	29.68	93.73
KLMatch [19]	51.22	85.12	56.04	85.45	61.08	83.86	13.68	96.32	49.90	85.62	31.38	91.93	43.88	88.05
ReAct [38]	<b>36.35</b>	91.17	34.55	93.22	<u>43.32</u>	<u>90.83</u>	5.61	98.94	<u>30.30</u>	93.40	<u>16.01</u>	96.88	27.69	94.07
ViM [42]	38.67	<u>91.38</u>	<b>32.47</b>	<b>93.41</b>	44.23	89.86	<u>1.40</u>	<u>99.68</u>	31.80	<u>94.05</u>	16.61	<u>97.10</u>	<u>27.53</u>	<u>94.25</u>
<b>Feature space methods</b>														
Maha [30]	<u>36.61</u>	<u>91.67</u>	35.37	92.89	46.08	89.55	<u>0.96</u>	<u>99.78</u>	30.45	<u>94.22</u>	<b>13.85</b>	<b>97.50</b>	27.22	94.27
KNN [39]	38.28	90.74	46.08	90.73	54.50	87.54	6.75	98.70	38.95	92.53	20.59	96.12	34.19	92.72
<b>WDiscOOD</b>	<u>36.58</u>	<b>91.79</b>	<u>32.62</u>	<u>93.34</u>	<u>43.74</u>	89.91	<b>0.89</b>	<b>99.81</b>	<b>30.15</b>	<b>94.36</b>	14.30	97.44	<b>26.38</b>	<b>94.44</b>

(b) ViT-B/16 [10].

Table 1: **Results on ResNet-50 [18] and ViT [10] classification models.** We test all methods on six OOD datasets and compute the average performance. Both metrics AUROC and FPR95 are in percentage. We highlight the best performance in bold, and underline the 2nd and 3rd ones. Our method consistently outperforms all classifier-dependent or feature-space baselines under both network architectures in terms of average performance.

**ID and OOD datasets** We follow recent work [25] to test on large-scale OOD detection task with ImageNet-1k [6] as the ID dataset. Six test OOD datasets are included in our evaluation, including: *SUN* [43], *Places* [47], *iNaturalist* [41], *Textures* [4], *ImageNet-O* [22], and *OpenImage-O* [42]. For the first three (*SUN*, *Places*, *iNaturalist*), we use the subset curated by [25] with non-overlapping categories *w.r.t* the ID dataset. Note that our evaluation is more comprehensive than previous OOD detection literature investigating ImageNet benchmark [42, 39], in the sense that they only adopt a subset of our OOD datasets. Utilizing a varied range of OOD data sources can encompass a wider range of distributional shift patterns, thus enabling a more comprehensive evaluation of OOD detection methodologies.

**Evaluation Metrics** We report the two commonly adopted metrics to evaluate the ability of a scoring function to distinguish ID and OOD data by related literature. The first is *Area under the Receiver Operating Characteristic Curve (AUROC)*. A threshold-free metric that measures the area under the plot of the true positive rate (TPR) against the false positive rate (FPR) under varying classification thresholds. The AUROC metric is advantageous as it is invariant to the ratio of positive sample number to that of negative sample, making it suitable for evaluating OOD detection task, where the number of ID and OOD samples is of-

ten imbalanced. Higher value indicates better performance. The second is *False positive rate at 95% true positive rate (FPR95)* (the smaller the better)

**Models Settings and Hyperparameters** We test on classification models for ImageNet-1k [6] with various backbones. The first is classic ResNet-50 backbone [18], the most widely applied convolutional neural network. The second is Vision Transformer (ViT), a transformer-based vision model that processes input image as a sequence of patches. Following [39], we adopt the officially released ViT-B/16 architecture that is pretrained on ImageNet-21k and finetuned for the classification task on ImageNet-1k.

For stand-alone visual encoders, we test with Supervised Contrastive (SupCon) [26] and Contrastive Language-Image Pre-Training (CLIP) [35] model. The former is optimized to encourage similarity between the embeddings of samples from the same class, while maximizing the distance between that for different classes. The latter is a multi-modality representation learning method, trained to pull together the features for matched image-text pairs, while push away that for non-matching pairs. For both encoders, we adopt ResNet-50 backbone with officially released weights. Different from [14], we discard the language encoder from CLIP and perform OOD detection only in the visual feature space. This removes the assumption of the availability of textural ID class name or description, which is not always feasible in real-world application. While both models utilize a projection head to a low-dimensional embedding space to formulate the training objectives, we leverage the backbone penultimate layer feature for better performance for OOD detection following [39].

Following ViM [42], we adopt different hyperparameter settings according to feature dimension. For ResNet-50 encoder with  $D = 2048$  dimensional features, we set the number of discriminants as  $N_D = 1000$  and the score weight in Eq. 11 as  $\alpha = 5$ . On the other hand, we adopt  $N_D = 500$  and  $\alpha = 1$  for ViT feature space of  $D = 768$  dimensionality. When performing Linear Discriminative Analysis, we sample  $N = 200,000$  training images that are evenly distributed among all ID classes for the estimation of statistical quantities, such as means and scatter matrices.

**Baseline Methods** We compare our method with nine baselines that derive scores from pretrained models without requiring network modification or finetuning. Seven logit/probability-space methods are included, involving *MSP* [20], *Energy* [32], *ODIN* [31], *MaxLogit* [19], *KL-Match* [19], *ReAct* [38], and *VIM* [42]. For ReAct, we use Energy+ReAct setting with truncation percentile  $p = 99$ . Two feature-space baselines are also compared with, involving *Mahalanobis* [30] and *KNN* [39]. For Mahalanobis method, we follow SSD [36] to directly apply the scoring

function on the final layer feature without input-precessing or multi-layer feature ensemble technique.

#### 4.1. OOD Detection Performance on Classifiers

We first present the OOD detection comparison with classification models based on ResNet-50 and ViT backbones. The results are tabulated in Tab. 1a and Tab. 1b, respectively. For all methods, we report both detailed results on each OOD dataset as well as the average performance. The best AUROC and FPR95 are shown in bold, and the second and third place are underlined. Our evaluation shows that, on average across all OOD datasets, WDdiscOOD exhibits superior performance compared to the baselines for both ViT and ResNet-50 models. This validates the efficacy of our OOD score function design.

**Consistency across OOD distributions.** Tajwar et al [40] shows on small-scale OOD benchmarks that existing OOD detectors do not have a consistent performance across OOD data source. The property is important as the OOD data distribution is unpredictable in the open world. We demonstrate that WDdiscOOD consistently achieves top performance across all OOD datasets. As an illustration, our approach achieves top-3 performance in 11 out of 12 metrics (2 - AUROC and FPR95 - for each of the 6 OOD datasets) when used with the ViT-B/16 model, with 6 of them being the highest compared to the baseline methods. The close ones are ViM and Maha (both achieve 7 top-3 including 2 top-1), but their top-1 results are achieved on the same dataset, whereas ours are on three. This indicates that by examining both discriminative and residual information, our method is capable of detecting a broader range of OOD patterns.

**Robustness across encoder architectures.** Another critical aspect of our OOD detector is its model-agnostic nature, as evidenced by its consistently high performance across different models. This highlights the ability of our approach to handle the diverse feature manifolds induced by distinct network architectures.

#### 4.2. Results on Contrastive Visual Encoders

In order to demonstrate the applicability of our method, we evaluate it on the SupCon [26] and CLIP [35] models to verify its applicability on modern visual encoders. Since classifier-dependent baselines are not applicable to the stand-alone visual feature extractors, we only compare with two feature-space baselines - Mahalanobis [30] and KNN [39]. The results are collected in Tab. 2. WDdiscOOD surpasses baselines on both models, suggesting that our method is more effective in identifying OOD patterns across the feature space induced by diverse representation learning objectives.

Method	SupCon [26]		CLIP [35]	
	FPR95↓	AUROC↑	FPR95↓	AUROC↑
Mahalanobis	46.95	89.78	78.00	75.31
KNN	42.51	90.35	82.59	67.22
<b>WDiscOOD</b>	<b>40.10</b>	<b>90.89</b>	<b>77.57</b>	<b>75.74</b>

Table 2: **Results on SupCon [26] and CLIP [35] visual encoders.** Our method surpasses other feature-space methods on these representation learning models. This table reports only average performance, while detailed results for each dataset can be found in the Supplementary material.

Method	ResNet-50		ViT	
	FPR95↓	AUROC↑	FPR95↓	AUROC↑
PR	56.72	84.01	34.59	92.44
<b>WDR</b>	<b>53.74</b>	<b>86.56</b>	<b>30.35</b>	<b>93.72</b>

Table 3: **Comparison between subspace techniques.** Our proposed WDR space is more effective than the Principle Residual (PR) space [42] for the OOD detection task. Furthermore, its AUROC on ResNet-50 outperforms 8 out of 9 baselines, which demonstrates that WDR is very informative for OOD detection task.

In order to demonstrate the applicability of our method on modern visual encoders, we evaluate it on SupCon [26] and CLIP [35] models. Since classifier-dependent baselines are not suitable for stand-alone visual feature extractors, we only compare with two feature-space baselines - Mahalanobis [30] and KNN [39]. The results, shown in Table 2, demonstrate that WDiscOOD outperforms both baselines on both models. This suggests that our method is effective in identifying OOD patterns from the feature space trained with diverse representation objectives.

### 4.3. Understanding WDiscOOD

**Discriminant Residual v.s. Principle Residual** We further demonstrate the efficacy of WDR space for OOD detection by comparing with other subspace residual design. ViM [42] bases their method on the residual of principle space, with empirical evidence on its effectiveness over classifier null space method [5]. We compare it against our residual score in Eq. 10 on the classification models. The results are shown in Tab. 3. Our designed scoring function in WDR space outperforms previous subspace technique in terms of AUROC and FPR95 for both ResNet-50 and ViT architectures. In addition, even *without* the discriminative information, it performs competitively compared to SOTA in Tab. 1. In particular, our WDR space score achieves the third highest AUROC on ResNet-50 classifier, only inferior to our integrated WDiscOOD score and Mahalanobis. This strongly supports our claim that WDR space is highly informative for OOD detection.

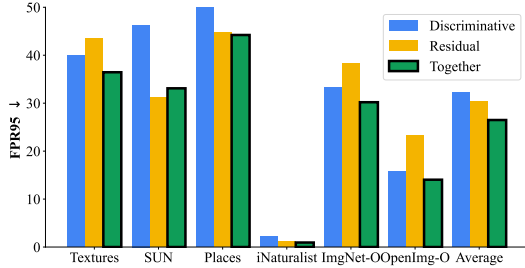
Config		ResNet-50		ViT	
Whiten <sup>†</sup>	Dist	FPR95 ↓	AUROC ↑	FPR95 ↓	AUROC ↑
✗	Maha	53.65	86.20	29.81	93.47
✗	Eucl	74.56	81.17	32.21	93.52
✓	Maha	49.85	87.23	26.60	94.40
✓	Eucl	49.86	87.23	26.49	94.41

Table 4: **Ablation on Data whitening.** <sup>†</sup>: The option of data whitening before DLA. Whitening the data prior to DLA improves over no whitening (✗+ Eucl) or whitening after DLA (✗+ Maha). Furthermore, with prior data whitening, Euclidean (✓+Eucl) performs similar as Mahalanobis (✓+Maha) while requiring less computation, which justifies our design.

**Effect of Feature Whitening** We evaluate WDiscOOD with or without feature whitening on ResNet-50 and ViT classification model. To isolate the effect of feature decorrelation on LDA, we also ablate on replacing Euclidean distance with Mahalanobis distance (whitening + Euclidean) in Eq. 9 and Eq. 10. The results are collected in Tab. 4. It shows that feature whitening improves the performance by a large margin. Replacing Euclidean distance with Mahalanobis after LDA slightly improves the results without whitening, but is insufficient to fill the gap. This suggests that feature whitening facilitates LDA to isolate class-specific and residual information, which is crucial for our method. Mahalanobis *after* WLDA has similar performance as Euclidean, but requires additional scatter matrices estimation in subspaces. Therefore our design is justified.

**Contribution by WD and WDR Spaces** To understand the role played by each subspace, we break down the scoring function and evaluate the OOD detection *solely* within WD or WDR, with Eq. 9 or Eq. 10 as OOD score, separately. The FPR95 performance is illustrated in Fig. 3. Our results demonstrate that two subspaces are effective in detecting different OOD patterns. Specifically, WD outperforms WDR on three OOD datasets (SUN, Places, INaturalist), while underperforming on the others (Textures, ImageNet-O, OpenImage-O). Additionally, the integrated score achieves better performance than each individual space on average, indicating that our method effectively leverages the complementary information provided by both subspaces. Unlike ViM [42], we combine the class-specific and class-agnostic information for OOD detection without relying on task heads, which improves its applicability.

**Effect of scale factor  $\alpha$**  We ablate on the scale factor  $\alpha$  in Eq. 11 on the ResNet-50 classification model. We fix the number of discriminants  $N_D = 1000$  and test with different scales from the set:  $\alpha \in \{0.01, 0.1, 0.5, 1, 2, 5, 10, 100\}$ . Fig. 4 depicts the average AUROC under varied scaling factor.



**Figure 3: The individual performance in WD and WDR space.** Our results demonstrate that two subspaces are effective in detecting OOD data from distinct distributions. Moreover, the integrated score (black border) yields a superior performance compared to each individual, evidencing that our method unifies class-discriminative and class-agnostic information.

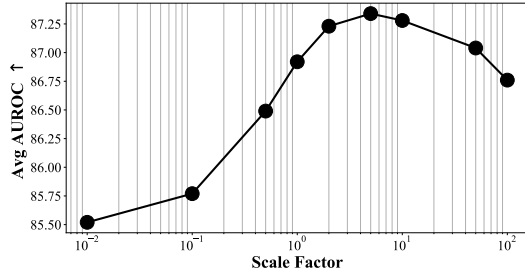


**Figure 4: Ablate on scoring scale factor.** The integrated performance is better than individual subspace over a wide range of scales, indicating that our simple linear combination is effective in factoring in information from both subspaces for OOD detection.

When the scaling factor is extreme, the score function biases towards one subspace over the other, leading to lower performance at both ends of the curve. Note that the integrated scoring function outperforms individual subspace score across a wide range of scales, indicating that albeit simple, the proposed linear combination is effective in factoring in information from both subspaces.

**Effect of Discriminant Number  $N_D$**  We also ablate on the effect of discriminant number  $N_D$ , by testing our method with  $N_D \in \{10, 100, 500, 1000, 1500, 2000\}$  on the same model. For each discriminant number, we test with varied scaling factor within the same set as above, and report the highest AUROC results. We further report individual performance from each subspace. The results are demonstrated in Fig. 5. As the discriminant number increases, *the individual performance in both WD and WDR space improves as the result of better separation between discriminative and residual information*. The trend stops when the number is sufficiently large, as the separation saturates. As a result, the intergrated performance becomes stable with increased discriminant number.

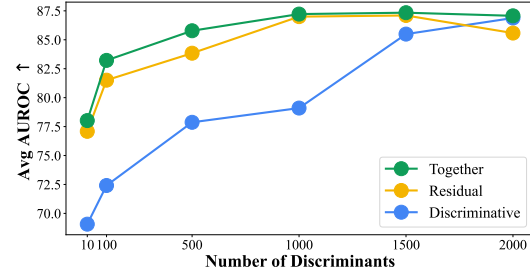


**Figure 5: Ablate on Discriminant Number  $N_D$ .** Our method achieves consistently high performance when the discriminant number is sufficiently large, enabling complete disentanglement of discriminative and residual information.

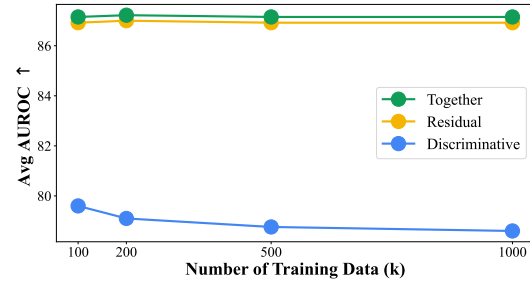


**Figure 6: Ablate on Training Data Number.** Our method achieves near-optimal performance using only 200K training data out of over 1000K, indicating that it is not excessively data-hungry.

**Robustness against Training Data Number  $N$**  Here we explore the effects of the training data number  $N$  on the performance of WDiscOOD. We vary the data number for parameters fitting, and plot the resulting average AUROC for individual subspace performance and integrated performance in Fig. 6. Near-optimal results can be achieved once 20% number of training data (200K out of over 1000K) is available, indicating the data efficiency of our method.

## 5. Conclusion

This paper presents a new OOD detection method based on Whitened Linear Discriminative Anaysis (WLDA), named WDiscOOD. It jointly reasons with class-specific and class-agnostic information by disentangling the discriminative and residual information from the feature space via WLDA. Comprehensive evaluation shows that our method establishes superior results on multiple large-scale benchmark, demonstrating robustness across model architectures as well as representation learning objectives. Our detailed analysis reveals the efficacy of Whitened Discriminative Residual Subspace (WDR) on OOD detection compared to other subspace techniques, showing the importance of understanding the behavior of OOD activation in the residual subspace.

## References

- [1] Abhijit Bendale and Terrance E Boult. Towards open set deep networks. In *IEEE/CVF Conference on Computer Vision and Pattern Recognition*, pages 1563–1572, 2016. 2
- [2] Paul Bodesheim, Alexander Freytag, Erik Rodner, Michael Kemmler, and Joachim Denzler. Kernel null space methods for novelty detection. In *IEEE/CVF Conference on Computer Vision and Pattern Recognition*, pages 3374–3381, 2013. 3
- [3] Ting Chen, Simon Kornblith, Mohammad Norouzi, and Geoffrey Hinton. A simple framework for contrastive learning of visual representations. In *International Conference on Machine Learning*, pages 1597–1607. PMLR, 2020. 2
- [4] Mircea Cimpoi, Subhransu Maji, Iasonas Kokkinos, Sammy Mohamed, and Andrea Vedaldi. Describing textures in the wild. In *IEEE/CVF conference on Computer Vision and Pattern Recognition*, pages 3606–3613, 2014. 5
- [5] Matthew Cook, Alina Zare, and Paul Gader. Outlier detection through null space analysis of neural networks. *arXiv preprint arXiv:2007.01263*, 2020. 2, 7
- [6] Jia Deng, Wei Dong, Richard Socher, Li-Jia Li, Kai Li, and Li Fei-Fei. Imagenet: A large-scale hierarchical image database. In *IEEE/CVF conference on Computer Vision and Pattern Recognition*, pages 248–255, 2009. 5, 6
- [7] Terrance DeVries and Graham W Taylor. Learning confidence for out-of-distribution detection in neural networks. *arXiv preprint arXiv:1802.04865*, 2018. 3
- [8] Akshay Raj Dhamija, Manuel Günther, and Terrance Boult. Reducing network agnostophobia. *Advances in Neural Information Processing Systems*, 31, 2018. 3
- [9] Matthias Dorfer, Rainer Kelz, and Gerhard Widmer. Deep linear discriminant analysis. *arXiv preprint arXiv:1511.04707*, 2015. 4
- [10] Alexey Dosovitskiy, Lucas Beyer, Alexander Kolesnikov, Dirk Weissenborn, Xiaohua Zhai, Thomas Unterthiner, Mostafa Dehghani, Matthias Minderer, Georg Heigold, Sylvain Gelly, et al. An image is worth 16x16 words: Transformers for image recognition at scale. *arXiv preprint arXiv:2010.11929*, 2020. 5
- [11] Xuefeng Du, Zhaoning Wang, Mu Cai, and Yixuan Li. Vos: Learning what you don’t know by virtual outlier synthesis. *arXiv preprint arXiv:2202.01197*, 2022. 3
- [12] J Duchene and S Leclercq. An optimal transformation for discriminant and principal component analysis. *IEEE Transactions on Pattern Analysis and Machine Intelligence*, 10(6):978–983, 1988. 3
- [13] Donald H. Foley and John W Sammon. An optimal set of discriminant vectors. *IEEE Transactions on computers*, 100(3):281–289, 1975. 3
- [14] Stanislav Fort, Jie Ren, and Balaji Lakshminarayanan. Exploring the limits of out-of-distribution detection. *Advances in Neural Information Processing Systems*, 34:7068–7081, 2021. 2, 6
- [15] Ian Goodfellow, Jean Pouget-Abadie, Mehdi Mirza, Bing Xu, David Warde-Farley, Sherjil Ozair, Aaron Courville, and Yoshua Bengio. Generative adversarial networks. *Communications of the ACM*, 63(11):139–144, 2020. 3
- [16] Chuan Guo, Geoff Pleiss, Yu Sun, and Kilian Q Weinberger. On calibration of modern neural networks. In *International Conference on Machine Learning*, pages 1321–1330. PMLR, 2017. 1
- [17] Bharath Hariharan, Jitendra Malik, and Deva Ramanan. Discriminative decorrelation for clustering and classification. In *Computer Vision–ECCV 2012: 12th European Conference on Computer Vision, Florence, Italy, October 7–13, 2012, Proceedings, Part IV 12*, pages 459–472. Springer, 2012. 4
- [18] Kaiming He, Xiangyu Zhang, Shaoqing Ren, and Jian Sun. Deep residual learning for image recognition. In *IEEE/CVF conference on Computer Vision and Pattern Recognition*, pages 770–778, 2016. 5, 6
- [19] Dan Hendrycks, Steven Basart, Mantas Mazeika, Andy Zou, Joseph Kwon, Mohammadreza Mostajabi, Jacob Steinhardt, and Dawn Song. Scaling out-of-distribution detection for real-world settings. In *International Conference on Machine Learning*, pages 8759–8773. PMLR, 2022. 1, 2, 5, 6
- [20] Dan Hendrycks and Kevin Gimpel. A baseline for detecting misclassified and out-of-distribution examples in neural networks. *International Conference on Learning Representations*, 2017. 1, 2, 5, 6
- [21] Dan Hendrycks, Mantas Mazeika, and Thomas Dietterich. Deep anomaly detection with outlier exposure. *arXiv preprint arXiv:1812.04606*, 2018. 3
- [22] Dan Hendrycks, Kevin Zhao, Steven Basart, Jacob Steinhardt, and Dawn Song. Natural adversarial examples. In *Proceedings of the IEEE/CVF Conference on Computer Vision and Pattern Recognition*, pages 15262–15271, 2021. 5
- [23] Yen-Chang Hsu, Yilin Shen, Hongxia Jin, and Zsolt Kira. Generalized odin: Detecting out-of-distribution image without learning from out-of-distribution data. In *IEEE/CVF Conference on Computer Vision and Pattern Recognition*, pages 10951–10960, 2020. 1, 3
- [24] Rui Huang, Andrew Geng, and Yixuan Li. On the importance of gradients for detecting distributional shifts in the wild. *Advances in Neural Information Processing Systems*, 34:677–689, 2021. 1, 2
- [25] Rui Huang and Yixuan Li. Mos: Towards scaling out-of-distribution detection for large semantic space. In *Proceedings of the IEEE/CVF Conference on Computer Vision and Pattern Recognition*, pages 8710–8719, 2021. 3, 5
- [26] Prannay Khosla, Piotr Teterwak, Chen Wang, Aaron Sarna, Yonglong Tian, Phillip Isola, Aaron Maschinot, Ce Liu, and Dilip Krishnan. Supervised contrastive learning. *Advances in neural information processing systems*, 33:18661–18673, 2020. 2, 6, 7
- [27] Balaji Lakshminarayanan, Alexander Pritzel, and Charles Blundell. Simple and scalable predictive uncertainty estimation using deep ensembles. *Advances in neural information processing systems*, 30, 2017. 2
- [28] Jinsol Lee and Ghassan AlRegib. Gradients as a measure of uncertainty in neural networks. In *IEEE International Conference on Image Processing (ICIP)*, pages 2416–2420, 2020. 1, 2
- [29] Kimin Lee, Honglak Lee, Kibok Lee, and Jinwoo Shin. Training confidence-calibrated classifiers for detecting out-

of-distribution samples. *arXiv preprint arXiv:1711.09325*, 2017. 3

[30] Kimin Lee, Kibok Lee, Honglak Lee, and Jinwoo Shin. A simple unified framework for detecting out-of-distribution samples and adversarial attacks. *Advances in neural information processing systems*, 31, 2018. 2, 5, 6, 7

[31] Shiyu Liang, Yixuan Li, and R Srikant. Enhancing the reliability of out-of-distribution image detection in neural networks. In *International Conference on Learning Representations*, 2018. 1, 2, 5, 6

[32] Weitang Liu, Xiaoyun Wang, John Owens, and Yixuan Li. Energy-based out-of-distribution detection. *Advances in neural information processing systems*, 33:21464–21475, 2020. 1, 2, 3, 5, 6

[33] Ibrahima Ndiour, Nilesh Ahuja, and Omesh Tickoo. Out-of-distribution detection with subspace techniques and probabilistic modeling of features. *arXiv preprint arXiv:2012.04250*, 2020. 2, 4

[34] Vo Dinh Minh Nhat, Sung Young Lee, and Hee Yong Youn. Whitened lda for face recognition. In *ACM international conference on Image and video retrieval*, pages 234–241, 2007. 4

[35] Alec Radford, Jong Wook Kim, Chris Hallacy, Aditya Ramesh, Gabriel Goh, Sandhini Agarwal, Girish Sastry, Amanda Askell, Pamela Mishkin, Jack Clark, et al. Learning transferable visual models from natural language supervision. In *International Conference on Machine Learning*, pages 8748–8763. PMLR, 2021. 2, 6, 7

[36] Vikash Sehwag, Mung Chiang, and Prateek Mittal. Ssd: A unified framework for self-supervised outlier detection. In *International Conference on Learning Representations*, 2021. 2, 6

[37] Mohit Shridhar, Lucas Manuelli, and Dieter Fox. Cliport: What and where pathways for robotic manipulation. In *Conference on Robot Learning*, pages 894–906. PMLR, 2022. 2

[38] Yiyou Sun, Chuan Guo, and Yixuan Li. React: Out-of-distribution detection with rectified activations. *Advances in Neural Information Processing Systems*, 34:144–157, 2021. 2, 5, 6

[39] Yiyou Sun, Yifei Ming, Xiaojin Zhu, and Yixuan Li. Out-of-distribution detection with deep nearest neighbors. *International Conference on Machine Learning*, 2022. 2, 5, 6, 7

[40] Fahim Tajwar, Ananya Kumar, Sang Michael Xie, and Percy Liang. No true state-of-the-art? ood detection methods are inconsistent across datasets. *arXiv preprint arXiv:2109.05554*, 2021. 6

[41] Grant Van Horn, Oisin Mac Aodha, Yang Song, Yin Cui, Chen Sun, Alex Shepard, Hartwig Adam, Pietro Perona, and Serge Belongie. The inaturalist species classification and detection dataset. In *IEEE/CVF conference on Computer Vision and Pattern Recognition*, pages 8769–8778, 2018. 5

[42] Haoqi Wang, Zhizhong Li, Litong Feng, and Wayne Zhang. Vim: Out-of-distribution with virtual-logit matching. In *IEEE/CVF conference on Computer Vision and Pattern Recognition*, pages 4921–4930, 2022. 1, 2, 4, 5, 6, 7

[43] Jianxiong Xiao, James Hays, Krista A Ehinger, Aude Oliva, and Antonio Torralba. Sun database: Large-scale scene recognition from abbey to zoo. In *IEEE/CVF conference on Computer Vision and Pattern Recognition*, pages 3485–3492, 2010. 5

[44] Jingkang Yang, Kaiyang Zhou, Yixuan Li, and Ziwei Liu. Generalized out-of-distribution detection: A survey. *arXiv preprint arXiv:2110.11334*, 2021. 1

[45] Qing Yu and Kiyoharu Aizawa. Unsupervised out-of-distribution detection by maximum classifier discrepancy. In *IEEE/CVF international conference on computer vision*, pages 9518–9526, 2019. 3

[46] Alireza Zaeemzadeh, Niccolò Bisagno, Zeno Sambugaro, Nicola Conci, Nazanin Rahnavard, and Mubarak Shah. Out-of-distribution detection using union of 1-dimensional subspaces. In *IEEE/CVF Conference on Computer Vision and Pattern Recognition*, pages 9452–9461, 2021. 3

[47] Bolei Zhou, Agata Lapedriza, Aditya Khosla, Aude Oliva, and Antonio Torralba. Places: A 10 million image database for scene recognition. *IEEE transactions on pattern analysis and machine intelligence*, 40(6):1452–1464, 2017. 5